

THIS ISSUE

The End of the Semiconductor Roadmap 1

Combining SEM with Chemical Imaging for Material Science 2,3

Microstructure Characterization of as-deposited Cu thin films on Si₃N₄ 4

We're on the Web
www.uwo.ca/fab

For More Information Visit Our Website

- Examples of work
- Contact Information
- Facilities Information
- How to become a NanoUser.
- Find out about services provided
- To subscribe or unsubscribe to NanoWestern

Questions & Comments?
Send them to:
nanofab@uwo.ca



WINS lecturer Eli Yablonovitch The End of the Semiconductor Roadmap. By Mitchell Zimmer

Prof. Eli Yablonovitch is the founding experimentalist in photonic band gap materials. The Professor of Electrical Engineering and Computer Science at UC Berkeley is known as being the first to design artificial crystal structures which manipulate light in a very special way. The new materials treat photons in a manner comparable to that of semiconductors controlling electrical signals through transistors. (There is even a crystal named after him called yablonovite.) These types of photonic crystals promise to revolutionize the information and telecommunications industries. Yablonovitch also had a hand in creating Luxtera. This is a company that has introduced an optoelectronic integrated cable capable of carrying data at rates up to 40 gigabytes per second.

As the 2008 Western Institute for Nanomaterials Science (WINS) Distinguished Lecturer, Yablonovitch gave a talk called "The End of the Semiconducting Roadmap: The Collision of Physics, Economics and Sociology." He provided a retrospective look at the growth, refinement and the various impacts of integrated circuits via silicon technology as well as a few predictions as to where the technology is going.

Yablonovitch often put the historical developments of semiconductors in context with his own life. He said that as a boy in the 1960's he would tinker with electronics, in one particular high school project he needed a few transistors. The problem was that the devices would cost nearly ten dollars apiece. One day, he found a mail order distributor who sold the components he needed for \$2.50 each. Yablonovitch admitted that "they were not NASA quality." Now it is possible for a single chip to contain over a billion transistors with each costing just a few millionths of a cent. During this same time period the number of transistors shipped went from a few billion in the late '60's to billions times billions in the present day. These observations are the real world consequences of Moore's Law what the co-founder of Intel Corporation, Gordon Moore, predicted in 1975.

Once the new technology has laid the foundation, other industries are built on top which manufacture devices, as well as programs and services running into trillions of dollars per year. As wondrous as these developments are, Yablonovitch raised the point that "when the industry becomes too successful, it becomes too efficient and what happens to industries like that is that they eventually shrink. I think of the agricultural industry. It used to be that in North America, a hundred years ago, half of all effort was in farming and then the farming got to be very efficient and now only one per cent of the effort is in farming." Yablonovitch says that the only way to prevent this from happening with semiconductors is that "you need to come up with new things, new functions, new unrecognized needs that people are willing to pay for. Once you've made the laptop too cheap then you have to have something beyond that."

Another challenge exists on the lower size limit that can be reached with semiconductors. The industry is already testing prototype transistors in the 9 nm (that's 9 billionths of a meter) range so that devices will be operating at the molecular level. This is the end of the roadmap predicted by Moore's Law. Nevertheless, there are technologies that are coming to fruition such as the growing popularity of wireless and multicore CPUs. Yablonovitch also predicted the rise of Radio Frequency ID chips, the shrinking of laptops down to the size of cell phones, the replacement of hard disks with flash technology, the refinements of speech recognition which will remove the need for keyboards and developing intelligent search engines.



On behalf of the staff at the Nanofabrication Laboratory, we would like to welcome Tim Goldhawk to the position of Laboratory Supervisor. Tim joins us with an extensive analytical chemistry background, which includes 16 years experience at the reference laboratory for one of the worlds largest animal feed manufacturers, Agribands Purina Canada. While at Purina, Tim helped to ensure the integrity of our food supply by performing all aspects of laboratory quality control analysis with a focus on metal spectroscopy. Be sure to stop by the lab, introduce yourself and join us in welcoming Tim.

Combining Scanning Electron Microscopy with Chemical Imaging for Materials Science



By Zhifeng Ding
Department of Chemistry, The University
of Western Ontario

Scanning electron microscopy (SEM) scans an electron beam focused on a specimen and measures the quantity of electrons scattered or emitted from the sample. The intensity of each successive point versus the coordinates of the scan area are plotted, which produces images of the sample surface with a resolution as high as 1 nm. One of the SEM microscopes in our Nanofab Laboratory is equipped with Energy dispersive X-ray spectroscopy (EDX). This is mainly used for the elemental analysis of a specimen because of its capability to detect characteristic X-ray uniquely emitted by an element's atomic structure bombarded by the electron beam.

Our Laboratory of Electrochemistry, Spectroscopy and Microscopy (<http://publish.uwo.ca/~zfding/>) has utilized SEM/EDX. Combining with our own chemical imaging tools, such as scanning electrochemical microscopy (SECM) and confocal Raman microspectroscopy (CRM), we have investigated surface reactivity of metal alloys^{1,2} and semiconductor nanostructures^{3,4}. One of our major goals is to bring insight into the relationships between structures and properties/functions of these materials.

Because of their excellent corrosion resistance, titanium alloys are well-studied candidates for the fabrication of engineered containers. However, information on chemical reactivity in micrometer scale for these materials is scarce. Nuclear power wastes are sealed in the containers prior to emplacement into selected repositories required to achieve containment for thousands to tens of thousands of years.

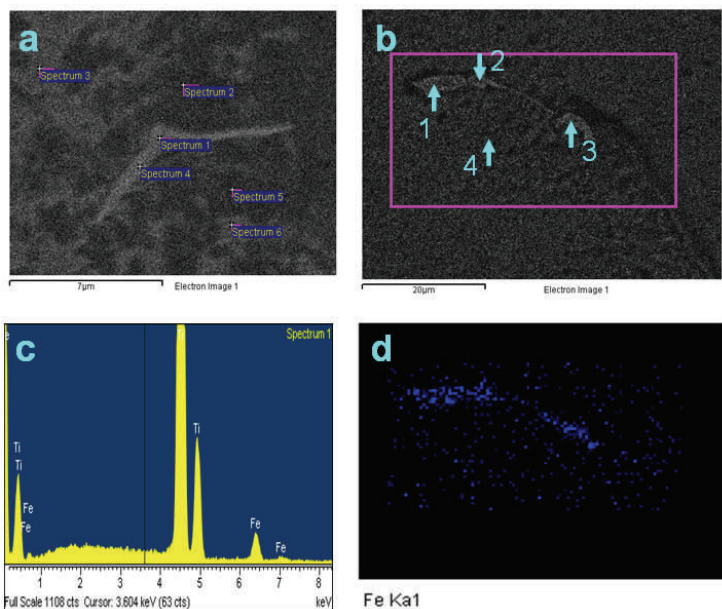


Figure 1. (a) A SEM image of a Ti-2 sample with visible grain boundaries. (b) Another SEM image with visible grain boundaries. (c) A typical EDX spectrum taken at position 1 in image b. (d) The EDX mapping of iron in the rectangular area shown in image b. The grain boundary at which Fe is accumulated in this image is very

ASTM Grade-2 titanium (Ti-2) was examined by the electron microscope in the Nanofab Lab (Leo 1540 FIB/SEM with Cross-Beam, Zeiss Nano Technology Systems Division, Germany)¹. SEM imaging, EDX analysis, and EDX mapping were carried out (Fig. 1). Figs. 1a and 1b illustrate the grain boundaries and triple points in Ti-2. The grain size was found to vary over the range of 20-100 nm and Fe contents in grains and at grain boundaries were observed in the range of 0.04 wt% and 10 wt%, respectively. It is evident that Fe is accumulated at the boundaries as shown by EDX mapping of Fe in Fig. 1d, given that Ti-2 contains 0.078 wt% Fe in average. SECM was utilized to map the reactivity of Ti-2 immersed in a 0.1 M NaCl solution (Fig. 2). Since Fe accumulated at the grain boundaries is expected to be more reactive than Ti, most active spots (blue spots) observed on the SECM images were proposed to be the triple points and, to a slightly lesser degree, the grain boundaries. To further demonstrate our point, the active spots were joined by black lines, which delineate the grain boundaries and triple points. The grain size measured in SECM images matched that determined by SEM.

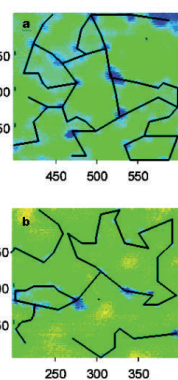
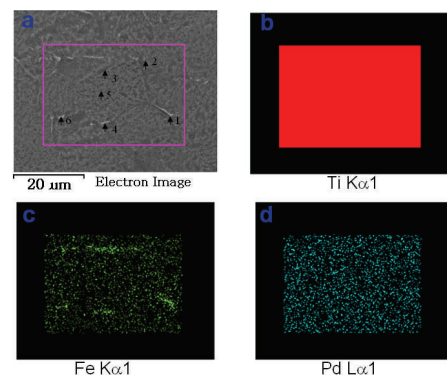


Fig. 2. SECM images with possible grain boundary structures on the Ti-2 surface. The blue spots are the active spots that appeared at the grain boundaries and triple points. The black lines were drawn by connecting the active spots, which represent the grain boundaries on the Ti-2 surface¹.

Fig. 3. SEM image (a) and EDX maps for Ti Ka1 (b), Fe Ka1 (c) and Pd La1 (d). The numbers labeled on image a indicate the points selected for EDX analyses of Pd and



SEM/EDX and SECM were further applied to analyze grain boundaries and the reactivity of a Ti-7 sample². The alloying element, Pd, and the impurity, Fe, were found to cosegregate to grain boundary locations using SEM (Fig. 3). The boundaries had a higher reactivity than grains, as assessed by SECM (Fig. 4). Further studies on Ti-12 and Zr alloys are being actively pursued in collaboration with Shoemith group.

SEM was used to characterize morphologies and chemical structures of single tin dioxide nanoribbons under ambient conditions³. SEM image of the SnO₂ nanoribbons indicated that the as-prepared nanoribbons are several tens nm in length, 100 nm to 1 μm in width and several tens nm in thickness. While some ribbons have a

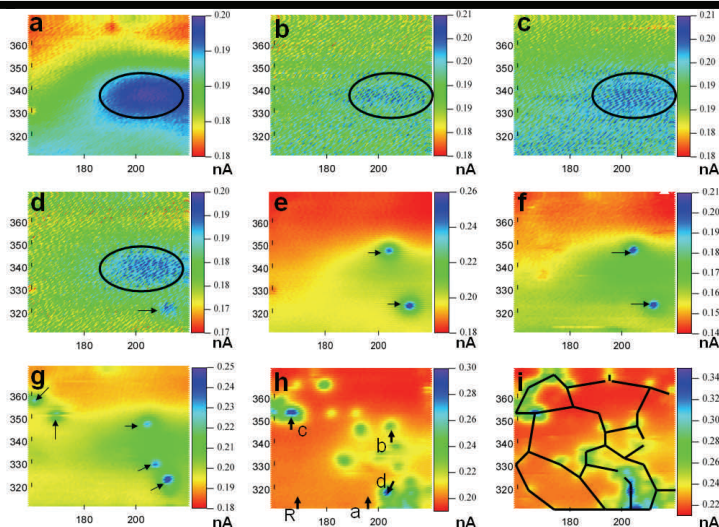


Fig. 4. SECM images of the same area of a Ti-7 surface biased at different potentials. The possible grain boundaries are shown on image *i*².

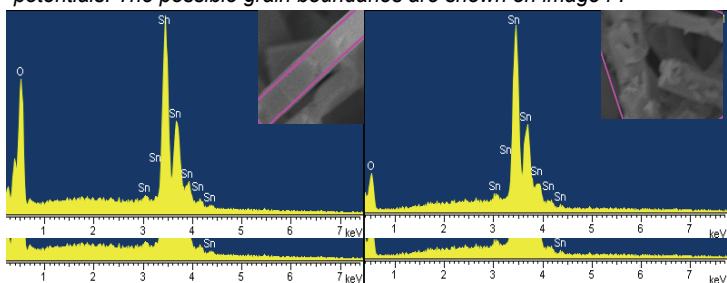


Fig. 5. The elemental composition of the SnO₂ nanoribbons with a smooth surface (left) and with extra nanostructures (right) analyzed by EDX³.

very smooth surface with a ratio of Sn to oxygen, 1:2, the second type of ribbon surfaces has the Sn:O about 1:1.43 which exhibits a considerable oxygen deficiency (Fig. 5). The two types of SnO₂ nanoribbons were further investigated by confocal Raman microscopy³. Showing a fundamental Raman peak at 633 cm⁻¹, the Raman spectrum of a single smooth SnO₂ nanoribbon confirms its rutile structure. Interestingly, Raman images illustrated that SnO_x (1 < x < 2) nanostructures grew on some SnO₂ nanoribbons³. The growth was caused by the defects of oxygen vacancy on surfaces of SnO₂. These nanostructures generated an additional group of very intense energy bands between 1000 and 1800 cm⁻¹. This is attributed to defect state SnO_x-like resonant emission and exciton-phonon coupling luminescence. One sharp peak at 170 cm⁻¹ with high intensity was observed in the Raman spectrum of ribbons with extra nanostructures, which could be ascribed to substoichiometric Sn₂O₃/Sn₃O₄ phases. Raman images constructed with the normal Raman band at 630 cm⁻¹, with the extra bands between 1000 and 1800 cm⁻¹ and the sharp peak at 170 cm⁻¹ (images in Fig. 6) firm up the above conclusions.

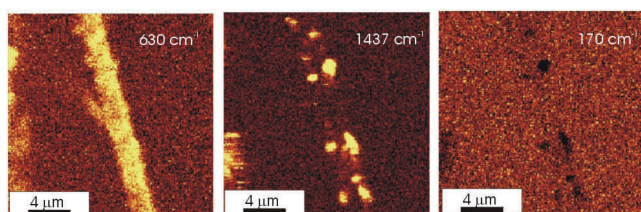


Fig. 6. Raman images of the SnO₂ nanoribbons³. (a) Raman image constructed with the normal Raman band at 630 cm⁻¹. (b) Raman image built with the extra bands between 1000 and 1800 cm⁻¹. (c) Raman image created from the peak at 170 cm⁻¹.

On the other hand, in collaboration with Drs. Tsun-Kong Sham and Xueliang Sun, we were able to trim down multiwalled carbon nanotubes to smaller nanostructures such as blue-luminescent nanocrystals, using electrochemistry⁴. The scanning electron microscope in the Nanofab has been used to monitor the fabrication processes ex-situ (Fig. 7)⁴. SEM is a versatile tool for our research on materials science.

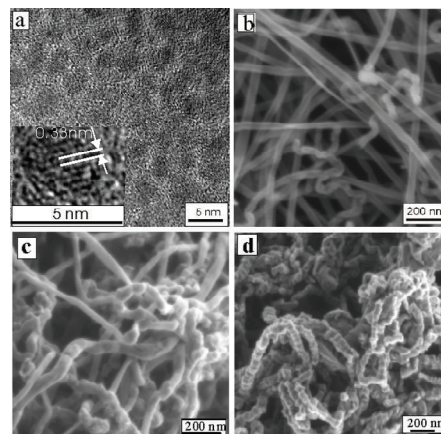


Fig. 7. HRTEM images of carbon nanocrystals (NCs) (a). SEM images of pristine carbon nanotubes (b); time-lapse change during the electrochemical treatment (c-d). Inset in a is the HRTEM image of a typical carbon NC⁴.

We appreciate the financial support for this research from Ontario Photonics Consortium, the Canadian Institute for Photonic Innovations, the Natural Sciences and Engineering Research Council of Canada, Canada Foundation for Innovation, Ontario Innovation Trust, the Premier's Research Excellence Award, and the University of Western Ontario. The Laboratory of Electrochemistry, Spectroscopy, and Microscopy is part of WINS and CCP at Western. Work from our research team Drs. Fengping Wang, Piotr Diakowski, Renkang Zhu, Jigang Zhou, Ms. Xiaocui Zhao, Ms. Catherine Nowierski, Ms. Christina Booker, and Kevin Daub is gratefully acknowledged. Thanks are owed to Drs. Rob Lipson, Tsun-Kong Sham, David W. Shoesmith, Jami Noel, Zack Qin, Ian Mitchell, Xueliang Sun, Silvia Mittler, Todd Simpson, Rick Glew, and Ms. Nancy Bell. Technique assistance from John Vanstone, John Aukema, Sherrie McPhee, Mary Lou Hart and Marty Scheiring is appreciated.

References

- (1) Zhu, R.; Nowierski, C.; Ding, Z.; Noel, J. J.; Shoesmith, D. W. *Chem. Mater.* **2007**, *19*, 2533-2543.
- (2) Zhu, R.; Qin, Z.; Noel, J. J.; Shoesmith, D. W.; Ding, Z. *Anal. Chem.* **2008**, *80*, 1437-1447.
- (3) Wang, F.; Zhou, X.; Zhou, J.; Sham, T.-K.; Ding, Z. *J. Phys. Chem. C* **2007**, *111*, 18839-18843.
- (4) Zhou, J.; Booker, C.; Li, R.; Zhou, X.; Sham, T.-K.; Sun, X.; Ding, Z. *J. Am. Chem. Soc.* **2007**, *129*, 744-745.

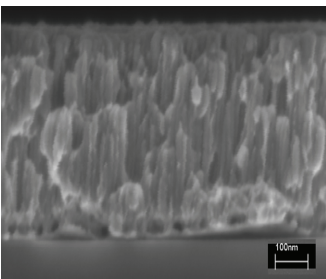
Microstructure characterization of as-deposited Cu thin films on Si₃N₄



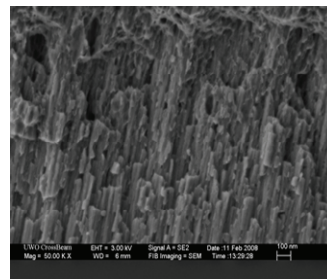
By Yong Liu (R.J. Klassen)
Department of Mechanical &
Materials Engineering
Faculty of Engineering
University of Western Ontario

Copper has high electrical and thermal conductivity and consequently better resistance to electromigration than other metals such as aluminum. Copper has, however, several inherent disadvantages, compared to aluminum which detract from its performance as an interconnect material in semiconductor applications. These disadvantages include the tendency to develop high residual elastic stress and incomplete surface passivation. To avoid potential reliability problems associated with Cu interconnects understanding the relationship between microstructural features, such as grain size, upon mechanical properties of Cu thin films is necessary.

The mechanical and electrical properties of thin metal films are largely governed by the metal deposition technique used in their fabrication. In this study, Physical Vapour Deposition (PVD) by ion sputtering was used to deposit Cu thin films of various thicknesses, between 200 and 3000 nm, on 100 nm thick Si₃N₄ windows supported in Si wafers. Cu films show a tendency to form textured columnar grained structures as shown by the fractographs in Figure 1. In order to confirm that the grain structure of the Cu was related to the columnar features shown in Figure 1, two TEM samples were made from Cu films of 823 nm and 1770 nm thickness. The LEO 1540XB Cross-Beam FIB/SEM at the UWO Nanofabrication Laboratory was used to create the TEM samples. A 1 nA 30 keV Ga⁺ ion beam was used to mill a tapered section of the Cu film such that the Cu thickness in the thinnest region was about 100 nm (i.e. transparent to 120 keV electrons).



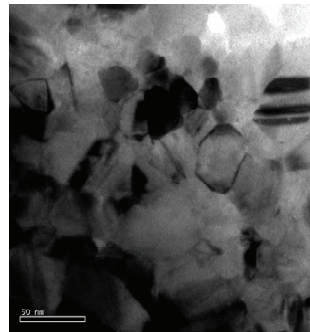
(a) 476 nm



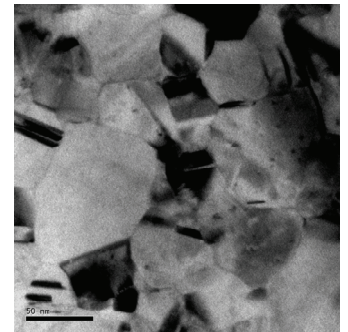
(b) 2656 nm

Figure 1 SEM side view images of the fracture surfaces as-deposited Cu films of two thicknesses.

TEM investigation of the prepared samples was then performed with a PHILIPS CM12 electron microscope (120 keV) at the Brockhouse Institute of Materials Research at McMaster University. Figure 2 shows TEM micrographs of the structure of the two as-deposited Cu films. The fracture surfaces shown in Figure 1 suggest an apparent difference in the columnar grain width between the two Cu film thicknesses. The average width of the columnar features on the fracture surfaces was 16.7 nm for the 476 nm thick Cu film and about 50 nm for the 2656 nm thick Cu film. The TEM micrographs (Figure 2) show that the grain shape, normal to the columnar features in Figure 1, is essentially equiaxed with an average grain diameter of 23.5 nm for the 823 nm thick Cu film and 41.3 nm for the 1770 nm thick Cu film. These results show clearly that the grain structure of sputter deposited Cu films is columnar, with equiaxed shape normal to the columns, and that the width of the columnar grains increases with increasing Cu film thickness. These results are important to my overall research objectives which are to investigate the effect of the microstructure on the creep deformation of Cu thin films both in the free-standing condition and when supported upon thin Si₃N₄ films.



(a) 823 nm



(b) 1.77 μm

Figure 2 TEM micrographs showing the grain structure, normal to the columnar features in Figure 1, of as-deposited Cu films of two thicknesses.

Acknowledgement:

The author wishes to thank Dr. Todd Simpson of the Nanofabrication Laboratory at The University of Western Ontario for making the TEM specimens and Mr. F. Pearson at McMaster University for assisting with the TEM.



The Nanofabrication Laboratory

University of Western Ontario
Physics & Astronomy Building Rm 14
London, Ontario N6A 3K7

Phone: 519-661-2111
Fax : 519-661-2033

Rick Glew, Lab Manager
Ext. 81458 Email: rglew@uwo.ca

Todd Simpson, Research Scientist
Ext. 86977 Email: tsimpson@uwo.ca

Silvia Mittler, Laboratory Director
Ext. 88592 Email: smittler@uwo.ca

Tim Goldhawk, Lab Supervisor
Ext. 81457 Email: tgoldhaw@uwo.ca

General Inquires Email: nanofab@uwo.ca

